EFFECTS OF MICROGRAVITY ON VISUAL IMPAIRMENT AND INTRACRANIAL PRESSURE SYNDROME

A Thesis
Presented to
The Academic Faculty

by

Sruti Bheri

In Partial Fulfillment
of the Requirements for the Degree
of Bachelor of Science in the
School of Biomedical Engineering

Georgia Institute of Technology
May 2017

EFFECTS OF MICROGRAVITY ON VISUAL IMPAIRMENT AND INTRACRANIAL PRESSURE SYNDROME

Approved by:

Dr. C. R. Ethier, Advisor
School of Biomedical Engineering
Georgia Institute of Technology

Dr. D. Tsygankov
School of Biomedical Engineering
Georgia Institute of Technology

Date Approved: May 5th 2017

To my fellow research students at the
Georgia Institute of Technology

ACKNOWLEDGEMENTS

I wish to thank Dr. C. Ross Ethier, Dr. Julia Raykin and the Ethier lab for the opportunity to participate in this research and the guidance and support throughout.

TABLE OF CONTENTS

LIST OF TABLES

LIST OF FIGURES

LIST OF SYMBOLS AND ABBREVIATIONS

Hcy	Homocysteine
ECM	Extracellular Matrix
ONS	Optic Nerve Sheath
VIIP	Visual Impairment and Intracranial Pressure
ICP	Intracranial Pressure
MRI	Magnetic Resonance Imaging
DMEM	Dulbecco's Modified Eagle's Medium
PCR	Polymerase Chain Reaction

CHAPTER 1

INTRODUCTION

When humans go into space for long durations, microgravity causes changes in the body. Recent long duration space flight has led to the observation of several new such adaptations of the body. One of the organs impacted by exposure to microgravity is the eye, in particular, the optic nerve (Nelson et al. 2014). Sixty percent of long-duration astronauts have reported alterations in their vision, a symptom of Visual Impairment and Intracranial Pressure (VIIP) syndrome (Gibson 2011). These ophthalmic changes, although initiated in space, persist after astronauts return to earth. Thus, a lot of recent biomedical space research deals with identifying the mechanisms causing these ocular changes in VIIP (Nelson et al. 2014). NASA has also given a high priority to understanding VIIP and developing mitigation methods for it (Marshall-Bowman 2011).

Previous research has shown that VIIP syndrome is influenced by several different ophthalmic conditions such as optic disc edema, choroidal folds, and cotton-wool spots (Nelson et al. 2014). Due to the diverse range of symptoms, it is difficult to determine the specific cause of VIIP. It is known, however, that the anatomical changes due to VIIP are similar to those seen in clinical patients on earth with intracranial hypertension (Marshall-Bowman 2011). Figure 1 shows the anatomy of the optic nerve (yellow) and the ONS surrounding it (white). The ONS

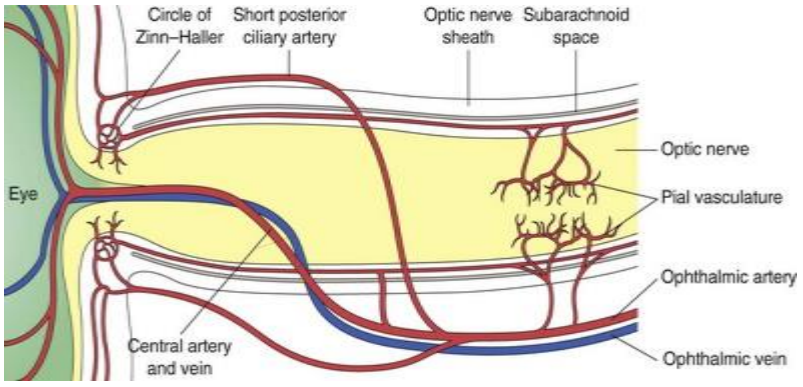

Figure 1. Optic Nerve Anatomy [Neuro-ophthalmology. (2015, October 3). Retrieved November 29, 2015, from http://clinicalgate.com/neuro-ophthalmology-2/]

contains the dura matter, pia matter and arachnoid matter and between these is the subarachnoid space which contains cerebrospinal fluid (Marshall-Bowman 2011). An increase in this cerebrospinal fluid volume is one cause for an increase in intracranial pressure (ICP). It is hypothesized that tissue remodeling, as a result of an increase in ICP in micro-gravitational conditions, contributes to the development of VIIP. It has been proposed that increases in ICP induce remodeling of the optic nerve sheath (ONS), which could lead to compression of the optic nerve. However, the effects of ICP on ONS remodeling have not been explored to date.

Our long-term goal is to study the biomechanical and cellular mechanisms of ONS remodeling. One aspect of the research shall be to determine the effect of ICP on ONS remodeling. Prior evidence also indicates that VIIP syndrome development correlates to an increase in serum concentrations of 1-carbon metabolites in astronauts (Gibson 2011). This is possibly due to enzymatic polymorphism in the 1-carbon metabolic pathway, leading to an increase of serum homocysteine (Hcy), a metabolite linked to neurological diseases and correlated with elevated cerebrospinal fluid volume. Due to this correlation, it is likely that an increase in Hcy could contribute to the development of VIIP syndrome. We wish to conduct ex vivo experiments on porcine ONS's to better understand the role of Hcy in VIIP. The *hypothesis* is that an increase in ICP and Hcy will synergistically cause the ONS to remodel after exposure to micro gravitational conditions.

The hypothesis shall be approached from two fronts. Firstly, the effect of Hcy (alongside increases in ICP) on the ONS shall be determined. To simulate increased cerebrospinal fluid pressure, the ONS will be attached to a pressure control system which will apply higher pressures to the ONS. This will be done in the presence and absence of Hcy to simulate increased Hcy effects. Tissue remodeling typically involves synthesis of additional extracellular matrix (ECM), increased protease production and reorganization

of ECM. These changes shall be observed by looking at collagen production, collagen microarchitecture and alterations in the stiffness and permeability of the ONS when exposed to increased ICP and Hcy. This will test if prolonged ICP and Hcy levels on the ONS cause remodeling. Secondly, computational models of the remodeling of the ONS to Hcy levels shall be created. The ONS will be modelled as a mixture of three materials: collagen, elastin and water. As each material's response to increased ICP and Hcy varies, their mechanical models will be independent of each other. This will allow for characterization of the ONS properties based on the stimuli.

This research will potentially help identify the cellular mechanisms involved in ONS remodeling. These ex vivo models will help identify and understand the mechanisms by which two of the contributing factors lead to the development of VIIP; increased ICP and Hcy. Understanding these factors will allow for future studies to be performed to mitigate them. The hope is that this in turn will reduce the cases of VIIP and prevent vision loss due to this condition in astronauts.

CHAPTER 2

LITERATURE REVIEW

Currently, research on VIIP and its causes is limited. However, recently more emphasis has been given to understanding the causes and manifestations of this syndrome. In a study performed by Dr. Robert Gibson, astronauts returning from a long duration in space were tested for visual acuity. A statistical analysis of the impact of VIIP on astronauts was conducted. One interesting observation was the correlation of VIIP with a variation in 1-carbon metabolic pathways in individuals. One limitation of this study was that only 7 patients were considered as the sample population for testing. The doctoral dissertation by Marshall-Bowman, in conjunction with NASA, further discussed several factors affecting VIIP. In-flight tests were performed that led to the recognition of a wider syndrome with the underlying cause possibly being an increase in ICP resulting in optic nerve distention. This paper cited several different possible causes of these bodily changes including an increase in ICP, carbon dioxide exposure limits, and sodium intake levels. Visual impairment could be influenced by several factors including cephalad fluid shift, exposure to high carbon dioxide levels, resistive exercise, high sodium intake and enzymatic polymorphisms. The study suggests that cephalad fluid shift, resistive exercise and high sodium intake likely contribute to an increase in ICP. More research is required to determine exactly how alterations in Hcy contribute to VIIP progression. More quantitative research is required to determine exact relationships between the factors aforementioned and their exact impact on visual acuity.

A review by Nelson et al. discussed further research the causes of ophthalmic changes due to long term space flight, more specifically, the effects of microgravity induced fluid shift on visual acuity. Theoretical analyses showed that the cephalad fluid shift impacted nerve distention. Due to the difficulty in mimicking space and microgravity conditions on

earth, most of their tests were limited to analysis of subjects already affected by VIIP. However, attempts were made to simulate microgravitational space conditions by performing the tests on negatively inclined beds where the lower-end of the bed was elevated higher than the head-end. This imitated the movement of fluid into the cerebral cavity due to microgravity. The study showed that 86% of the subjects presented cases of nerve sheath distention and nerve fiber layer thickening. These results triggered further research into the optic nerve and effects of pressure changes on the ONS shape and function.

One study that looked into the ONS shape was by Hansen et al. This study tested if O diameter could be a predictor for elevated ICP. A quantitative relationship between ONS diameter and increased sub-arachnoid pressure was established. The distensibility and elastic characteristics of the optic nerve sheath were measured by B-scan ultrasound in isolated human optic nerves. Following submission to pressure it was observed that 'the diameter of the ONS increased up to 140% of its baseline value'. Another important finding was that the sheath diameter might be irreversibly impaired after several episodes of prolonged intracranial hypertension and that the anterior ONS could be sufficient to measure changes in ICP.

When studying the ONS and specifically ONS diameters as performed by Hansen et al., the techniques used to perform the experiments become significant. Previous studies were conducted on porcine eyes and on cadaveric eyes but to understand the effects of ICP on VIIP patients, techniques to observe and measure the ONS in vivo are required. A couple of methods have been used for this purpose. One method is using magnetic resonance imaging (MRI) to specifically image intracranial and intraorbital abnormalities (Krammer et al. 2012). In the study performed by Krammer et al. both optic nerve and ONS diameters were measured by using three-dimensional data set visualization. Results

showed that the MRI technique gave reasonable images in 2D for reading the diameter of the ONS. Studies showed that ONS diameter values between 5-6mm are predictive of intracranial hypertension. Using MRI Krammer et al. found that a diameter of more than 5.82 mm related to cases of intracranial hypertension which supports the previous statement. This shows the reliability of this technique which could be useful for further quantitative studies on elevated ICP.

All the studies have focused on the structural and mechanical effects of the pressure on the optic nerve. The possibility that elevated ICP is related to vision changes has been brought forward and methods to conduct the research through different non-invasive imaging techniques have been discussed. The focus of the current study shall be on the *biological* factors affecting ICP. This study will more specifically determine if Hcy, alongside increased ICP, is a predisposing factor of VIIP. This is an aspect that has not been covered in previous literature but has been mentioned briefly in Gibson et al. The aim of this study is to further understand VIIP syndrome by checking if increased ICP and Hcy synergistically lead to VIIP contributing factors.

CHAPTER 3

METHODS

Tissue remodeling is normally a result of a change in the surrounding environment. This remodeling can therefore be detected and quantified based on the responses of the tissue milieu including ECM changes, DNA/RNA modifications and enzyme activity alterations. In this study, techniques were used to look at RNA expression, ECM protein expression and protease activity in ONS cells in response to changes in mechanical stretch and Hcy concentrations.

Optic nerve sheath (ONS) harvest and homogenization: Porcine eyes were obtained from a local abattoir (Holifield farms) less than 24 hours after animal death (Figure 2). The optic nerve was cut as close to the sclera as possible (~1-2mm) and the ONS (dura) was gently peeled. The ONS was then sterilized and stored in liquid nitrogen to maintain the structural integrity of the ONS. If immediately being treated with Hcy, the sheaths would be taken to the cell culture hood for treatment. A careful account of each ONS was maintained for future reference. Based on requirement, the tissue was then collagenase treated to obtain the ONS cells which were either used for experiments or stored in liquid nitrogen until required. For assessing protein and protease activity, whole ONS were treated with Hcy and exposed to 10% or 20% stretch after which they were homogenized in a homogenizer in 4°C.

Figure 2: A mounted porcine eye: showing the eyeball and the optic nerve prior to dissection.

ONS treatment with Hcy and Stretch:

The ONS cells were thawed from the liquid nitrogen and seeded into 6-well plates with

Dulbecco's Modified Eagle's Medium (DMEM) and 10% FBS. After 24 hours, the media was removed and replaced with DMEM containing pre-determined molarities of Hcy. For this, L-homocysteine or D,L-homocysteine was prepared fresh for each experiment by diluting the Hcy in phenol free DMEM with 1x penicillin-streptomycin.

When mechanical stretch was also being tested, the ONS cells were seeded onto 7.4cm x 4.1cm silicone strips and either placed in petri dishes (static) or placed on a uniaxial stretch system and exposed to 10 or 20% stretch for 24 hours. The conditions tested are shown in the table below (Table 1).

After the completion of the treatment, the cells were taken down from the 6-wells or silicone sheets and prepped for confocal microscopy, PCR, flow cytometry or zymography.

Table 1: Different Hcy and stretch conditions that were tested.

	Hcy Concentrations	Stretch
Conditions were different combinations of the 6 options shown:	0 Hcy	0%
	100µM Hcy	10%
	1000µM Hcy	20%

Zymography: MMP zymography was used to quantify protease activity. The treated samples of ONS were homogenized and their protein concentrations determined with a BCA kit. Once the gelatin-based SDS polyacrylamide gels for MMP-detection were made, equal amounts of protein were added to each gel lane. After the electrophoresis, the enzymes were renatured and the gels were incubated overnight so the gelatin could be digested by the enzymes. The gels were then submerged in 10% trichloroethanol so the protein bands can be detected via UV imaging. The gels were later immersed in Coomassie Blue followed by destain solution so the transparent bands of protease activity could be visualized against the blue background of the gel. The bands were then analyzed

through image analysis software using ImageQuant.

Histology: Sections of the ONS or portions of the ONS cell-seeded silicone were fixed in 4% paraformaldehyde. These samples were then stained for the desired proteins overnight. DAPI and phalloidin stains were also added to gauge the morphology of the cell and to provide reference. The samples were then imaged on a Zeiss 710 confocal microscope.

Flow Cytometry: The ONS cells were permeablized with saponin and treated with the required primary and secondary antibodies to detect fibronectin and vimentin. The samples were then run on a flow cytometer to quantify the amount of target proteins present in each condition.

CHAPTER 4

RESULTS

Determining the Variation of ONS Protein Concentrations to Changes in L-Homocysteine Concentration

The initial step was to determine the effect of physiological L-homocysteine concentration on several ECM protein concentrations. Reverse Transcriptase Polymerase Chain Reaction (RT-PCR) was performed to amplify RNA isolated from various ECM proteins of ONS cells. Figure 3 shows the RNA expression for fibronectin (FN), elastin (ELN1,2), laminin (Lam), collagen (Col1,3,4), connective tissue growth factor ß, (CTGF-b) and tissue growth factor (TGF). Aside from the variation in Hcy concentration, the effects of low and high glucose levels in the DMEM media were also investigated (Figure 3). Under low glucose conditions it appears that 5-100uM Hcy induces the maximum RNA expression for most proteins. Contrastingly, under high glucose conditions, 0uM Hcy seems to induce the largest RNA expression. Therefore, no distinct trend could be observed in low or high glucose media nor with the variation of Hcy.

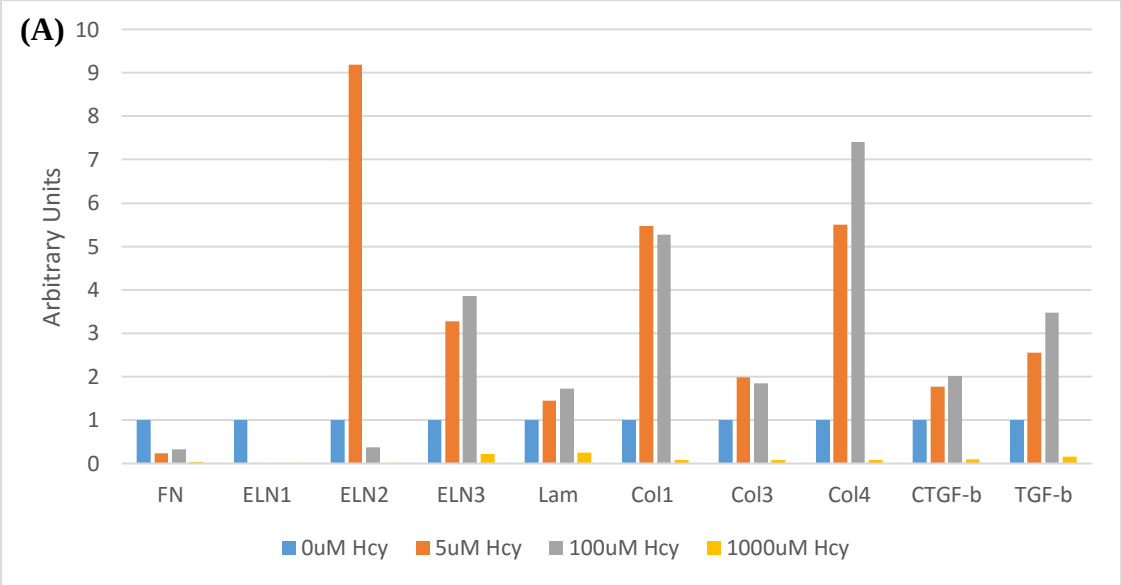

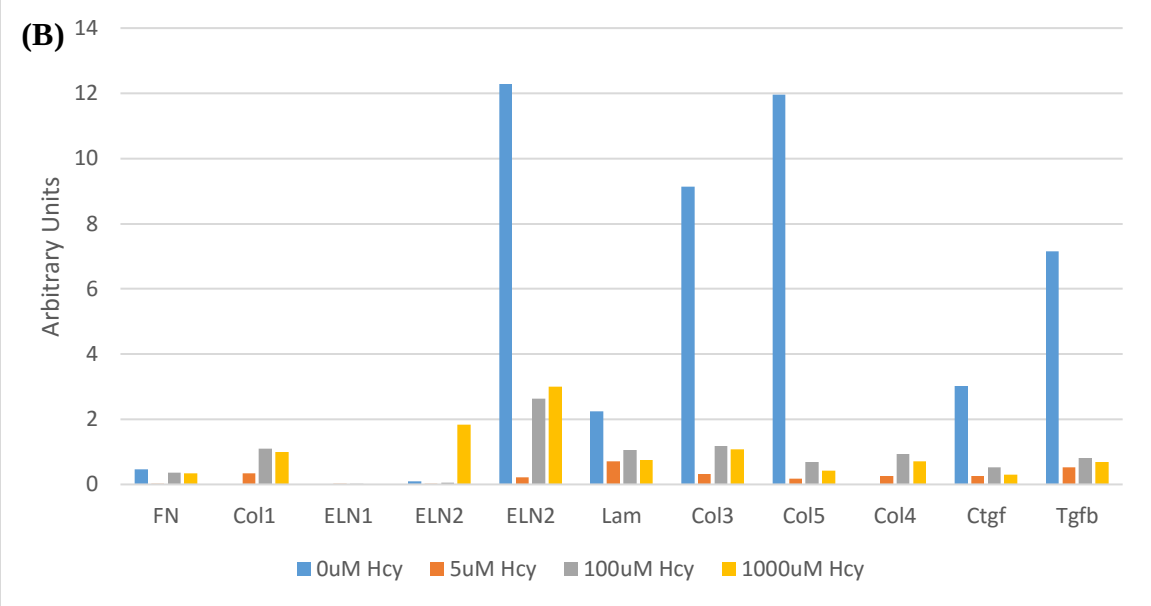

Figure 3. The effect of homocysteine and glucose concentrations on extracellular protein RNA expression. A: Low glucose (1g/L) in DMEM **B:** High glucose (4.5g/L) in DMEM. Data is normalized to the low glucose, 0 Hcy condition.

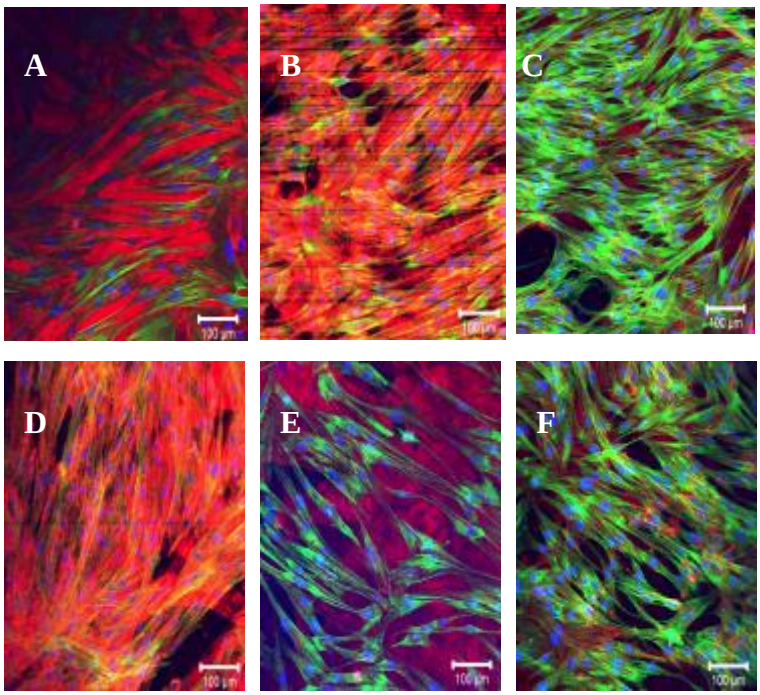

Figure 4: Confocal Microscopy of variations in fibronectin (red) expression with uniaxial stretch and homocysteine. A,B,C: 0µM Hcy with static (A), 10% stretch (B) and 20% stretch (C).**DEF:** 100µM Hcy with static (D), 10% stretch (E) and 20% stretch (F). Green = Phalloidin, Blue = DAPI. It should be noted that Figure 4b contained artifacts because of the imaging process, the horizontal lines were not part of the original sample.

Effect of uniaxial stretch and L-homocysteine on fibronectin expression

Based on the RT-PCR results, it was not evident that low or high glucose influenced the ECM protein concentrations. To simulate the effects of increased ICP on the ONS due to cerebrospinal fluid shifts, mechanical stretch was imparted on the ONS cells to see its effects. Here, uniaxial stretch conditions of 10% and 20% stretch were compared to the static case. Hcy concentrations were kept within the physiological range so only 0 and 100µM Hcy was used. The results were visualized through confocal microscopy by observing changes in the ECM protein, fibronectin (Figure 4).

Effect of uniaxial stretch and D,L-Homocysteine on Fibronectin and Vimentin Expression:

Since no differences between L-Hcy and D,L-Hcy were observed via PCR and because of the high cost of obtaining L-Hcy, D,L-Hcy was used in the remainder of this study. Moreover, mechanical stretch was imparted on the ONS cells to determine if there was a combined effect (Figure 5) on fibronectin and vimentin expression. Again, the same four concentrations of Hcy were used despite 1000uM Hcy being far beyond the concentration required for ONS damage. Flow cytometry was performed to observe the effect of Hcy and stretch on two ECM proteins (fibronectin and vimentin).

(A)

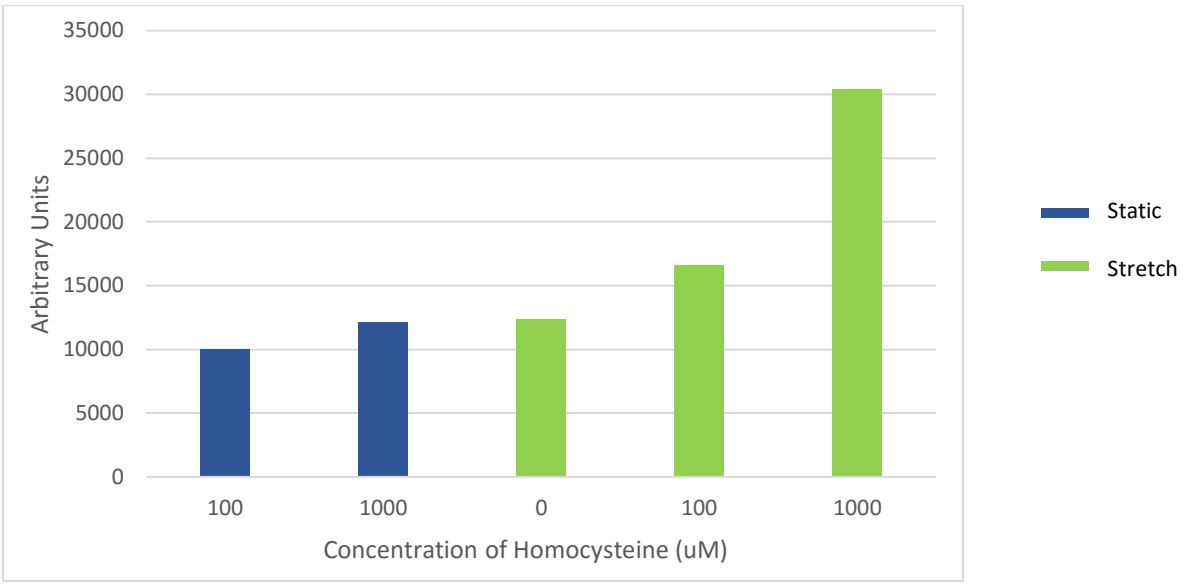

(B)

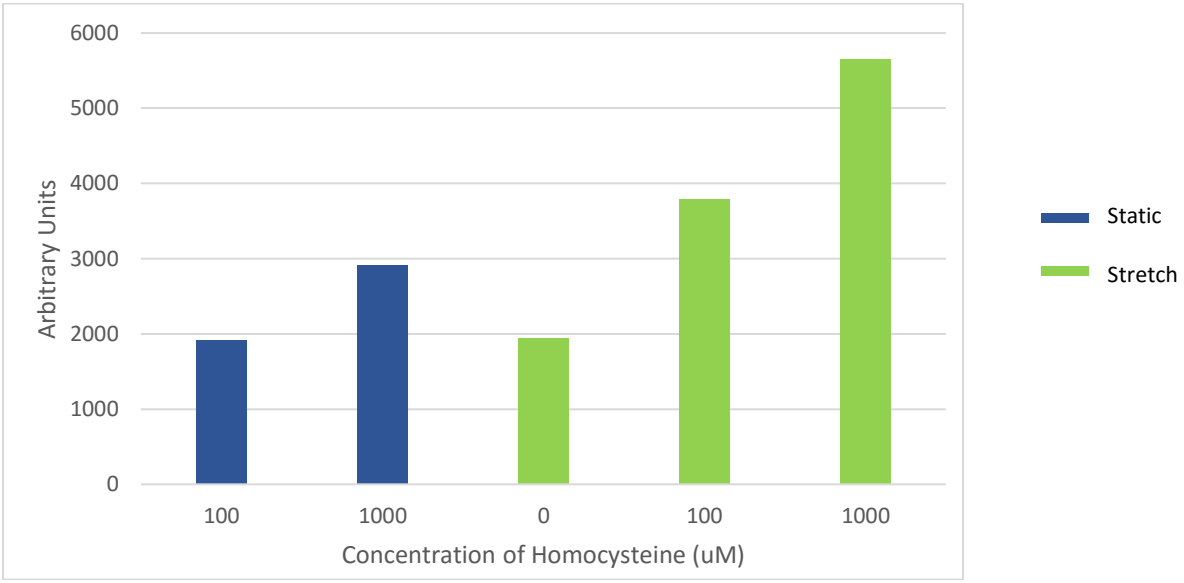

Figure 5. The effect of D,L-homocysteine and uniaxial stretch on extracellular protein concentration.
A: Fibronection **B:** Vimentin

Total Protein Normalization for Zymography

To determine the effects of Hcy and mechanical stimulation on protease activity, gelatin zymography was performed. However, current zymography techniques do not use a standard normalization technique. To facilitate normalization of enzyme activity, we devised a protocol which uses 2,2,2-tricholoroethanol (TCE). TCE is commonly used in western blots for band normalization. To determine its usage for zymography, the first

step was to determine the time period to incubate the zymography gels in TCE prior to UV exposure. Figure 6 shows that the protein intensity remains relatively constant for the first 10 minutes beyond which there is a drop of intensity. It can therefore be concluded that 10 minutes or less exposure to TCE is ideal for protein normalization.

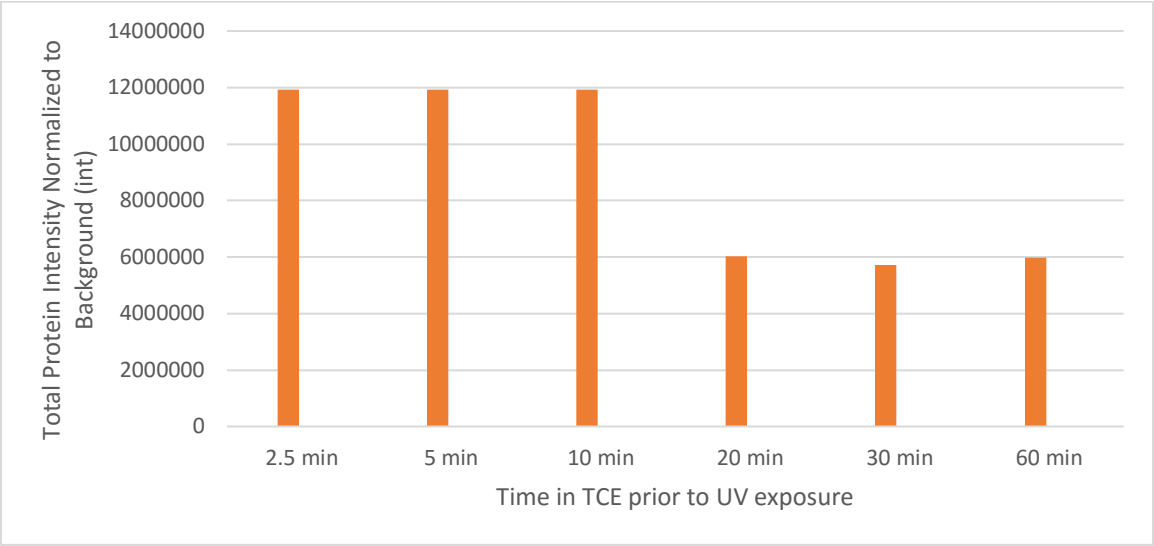

Figure 6. Optimum TCE Incubation Time for Protein Normalization. Measured on the Western Blot imager with 2.5 minute UV exposure.

The next step was to show that both gelatinase activity and total protein could be visualized on the same gel. Total protein signal was successfully measured with no detectable background signal (Figure 7a) and all the bands were evident. Once the Coomassie Blue Stain was added, it was also possible to detect the white bands where the gelatin had been digested and the total protein signal was no longer visible (Fig 7b). TCE signal increased linearly with total loaded protein (Figure 7c), and this was akin to what has previously been shown in western blots. Based on the location of the gelatin bands on the gel, it could further be determined that, matrix metalloproteinase(MMP)-2 activity also increased linearly until saturation was reached at approximately 15 µg of loaded protein per lane (Figure 7d).

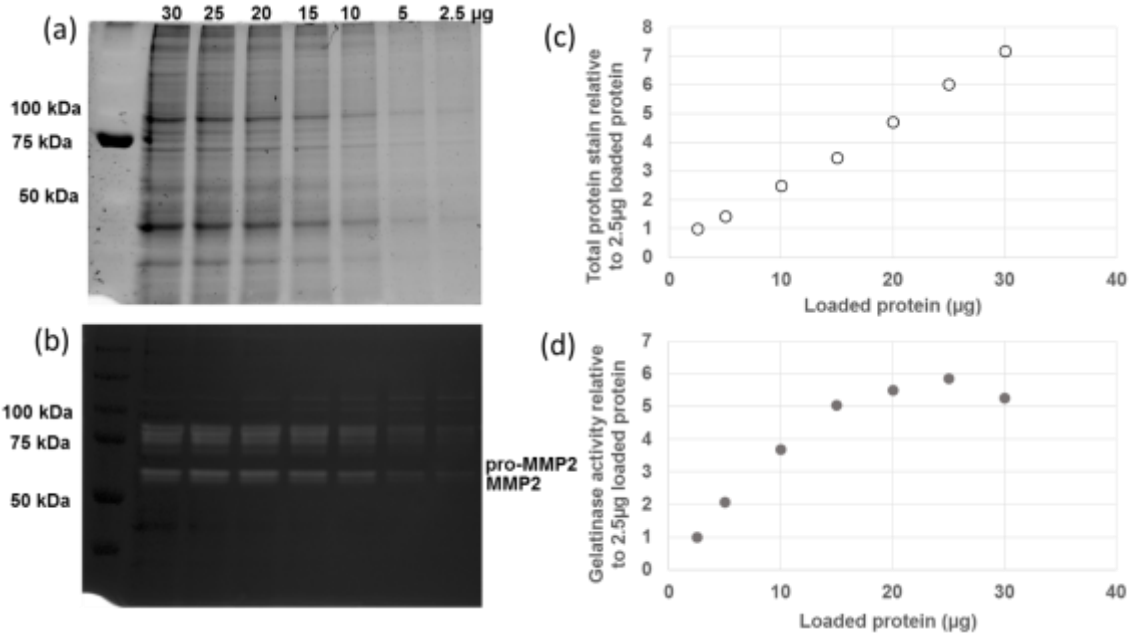

Figure 7. a: Total protein visualized with TCE in a polyacrylamide gel with a gelatin substrate. Values at the top of each lane indicate the nominally loaded mass of protein **b:** Zymogram indicating gelatinase activity in the same gel. Plots showing **c:** the TCE fluorescent intensity and **d:** the total gelatinase activity

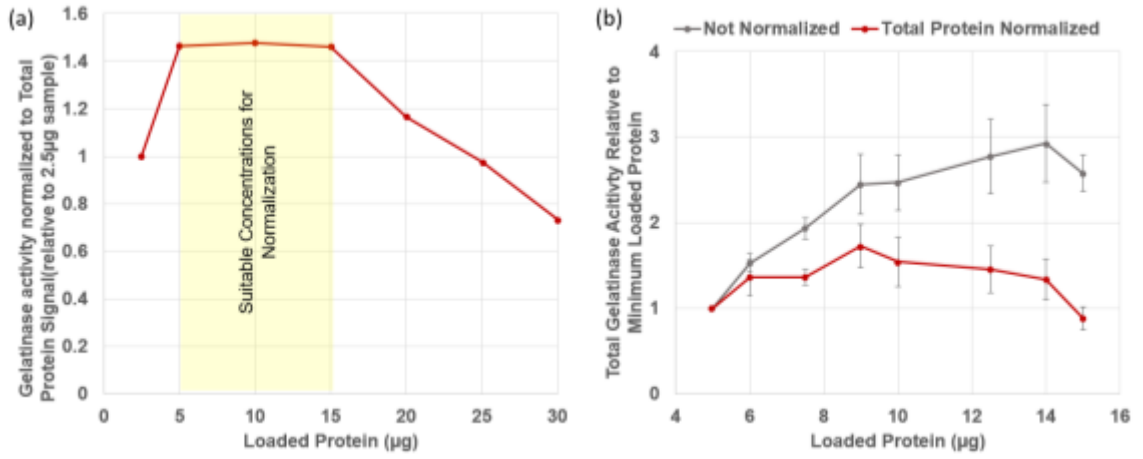

Figure 8. a: Gelatinase activity (loaded from 2.5-30 µg) normalized by total protein. The yellow-shaded region is the range where normalized gelatinase activity was approximately constant. **b:** Total gelatinase activity within yellow-shaded concentration range from panel (a), with and without total protein normalization (n=3, error bars denote standard deviation). Coefficients of variation (standard deviation divided by the mean) were 0.3 and 0.2 for not normalized and total protein normalized, respectively.

The final stage was to determine a suitable range within which the TCE normalized data was functional. This region was outlined to be the region in which the normalized activity

did not vary by a large degree (Fig 8a). As seen in the figure, this range falls between 5 - 15 µg of loaded protein per lane. It was found that at higher protein loading concentrations, the signal became saturated and at lower loading concentrations there was insufficient protein signal or enzyme activity to be detected and normalized. Further testing was then performed using 8 protein loading levels in the predetermined 5-15 µg protein per lane range. When the TCE normalization was performed, the enzyme activity was nearly constant between different loading conditions (Figure 8b). However, it should be noted that the non-normalized gelatinase activity kept increasing as the protein loading increased.

Effect of Hcy on ONS protease activity

To determine the activity of proteases in the ONS in response to different concentration of homocysteine, zymography with total protein normalization was performed. Specifically, variations in matrix-metalloproteinases (MMPs) were observed for different Hcy concentrations. High and low glucose conditions were also tested for two ONS samples. The trends observed showed that in almost all cases, MMP 9 was the most prominent band. However, the size of the MMP 2 band vs. the pro-MMP 2 varied significantly between experimental samples (Figure 9).

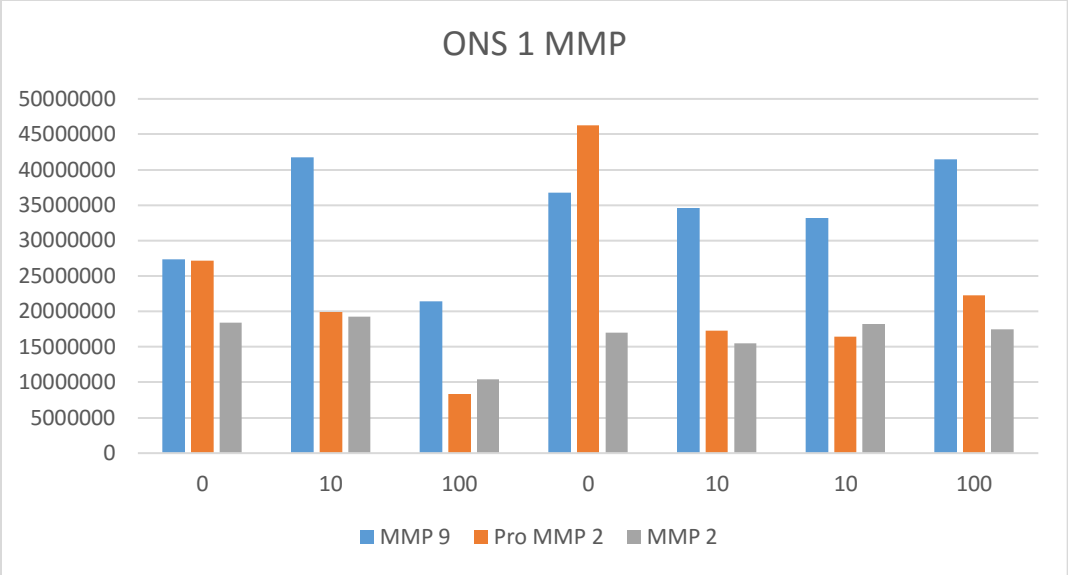

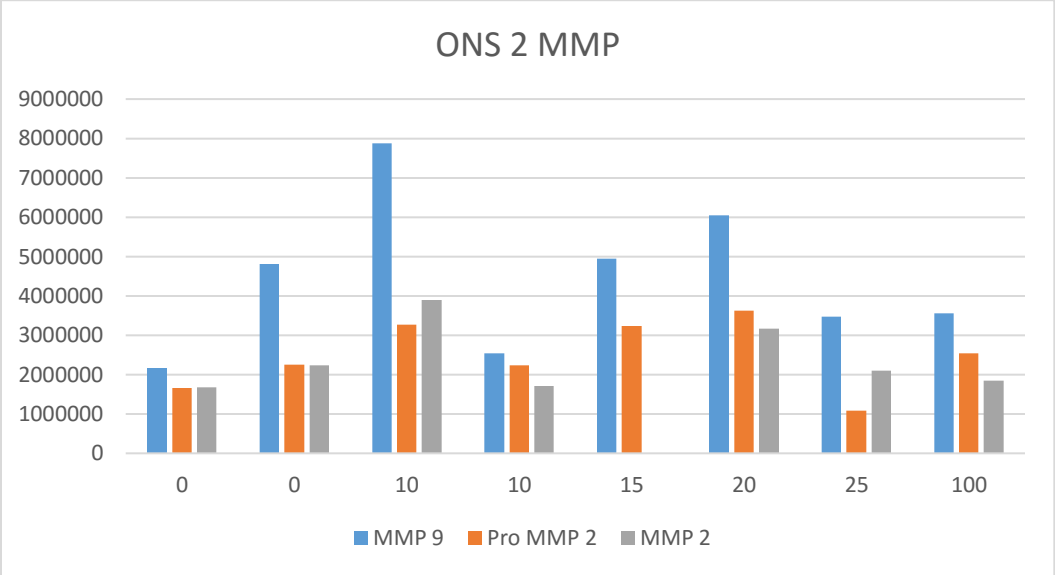

Figure 9: Plots of MMP band intensity showing MMP 2 and 9 and the effect of Hcy variation on MMP activity. ONS 1: lanes 1-3 = low glucose, lanes 4-7 = high glucose. **ONS 2:** lanes 2 and 5 = low glucose, rest of the lanes = high glucose.

CHAPTER 4

DISCUSSION

This study suggests that low and high glucose media have different impacts on the effect of Hcy. In addition, the effect of uniaxial stretch on the ONS cells was also studied. Aside from this, we were also able to develop a suitable protocol to normalize total protein during zymography and apply that to our experiments to understand the effect of Hcy and stretch on protease activity.

RT-PCR Protein Expression

Running RT-PCR allowed us to identify the complex effect that glucose and Hcy concentration had on protein expression. Under low-glucose conditions it appeared that 5uM Hcy induced the maximum protein expression for elastin whereas 100uM had a larger impact on collagen and the tissue growth factors. It is to be noted that for a few proteins 5uM and 100uM Hcy resulted in similar protein expression despite there being a 20-fold difference between the two concentrations. Moreover, under high glucose conditions, 0uM Hcy had the maximum impact on elastin, collagen and tissue growth factors. This suggests that the effect of the Hcy metabolite is dependent on glucose concentration. As VIIP patients often present with elevated blood glucose levels, we anticipated that higher glucose levels would correspond to higher Hcy concentrations (Marshall-Bowman 2011). The RT-PCR experiment, however, does not align with this.

Confocal Microscopy

The confocal microscopy data shows a qualitative representation of the combined effects of L-homocysteine and mechanical stretch on fibronectin. The amount of fibronectin decreased as stretch was applied and further as the applied stretch increased (Fig. 4a, 4b, 4c). Moreover, for a given amount of uniaxial stretch, an addition of Hcy also reduced the fibronectin expression (Fig 4a, 4b, 4c vs. 4d, 4e, 4f). This suggests that Hcy and mechanical stretch have a subtractive effect on the amount of fibronectin present on the ONS cell membrane.

Flow Cytometry

D,L-homocysteine resulted in increased concentrations of fibronectin and vimentin with stretch further increasing the protein expression. This coincided with the expected trends. However, this experiment was performed with 1000uM Hcy which is several orders more concentrated than would be found in the body. Therefore, despite the trends supporting our initial hypothesis, further study is required to determine if a significant trend is persistent at lower concentrations of Hcy (e.g. 5uM-100uM). Additionally, a baseline control of 0uM static should be included to confirm the data is significantly different.

Modified Zymography Protocol

Gelatin zymography was performed to study the effects of Hcy on protease activity. Traditional zymography techniques detect enzyme activity but provide minimal normalization to protein loading. Therefore, if more protein was accidentally loaded into one lane, the enzyme activity for that lane cannot be normalized to account for the excess protein. The modified protocol successfully achieves this goal through the addition of

TCE prior to Coomassie staining. This allows the total protein bands to be imaged and quantified prior to assessing enzyme activity so accurate protein normalization is possible. This allowed us to study the effect of Hcy on enzymatic activity and to study how the rate of protein expression varies within the ONS cells.

Protease activity

The MMP activity as seen in Figure 9 suggests that the most prominent enzyme activity in ONS cells is MMP 9. However, it is difficult to determine trends based on the plots. For ONS 1 it appears that for low glucose conditions, the peak MMP-9 activity was in the mid-range for 10μM Hcy, but for high glucose conditions, MMP-9 was always relatively high with the peak value at 100μM Hcy. A different case was seen in the second ONS sample for which high glucose conditions peaked around 10μM Hcy. However, it is evident that there is a lot of variation within a sample as ONS 2 had two samples at 10μM Hcy but their bands readings were more than 2-fold different from each other. Therefore, this data is inconclusive and further experiments must be performed before any trends can be deduced.

CHAPTER 5

CONCLUSION

The results from this study suggest that there are differences in protein expressions, protease activity and RNA expression for different levels of Hcy, glucose and mechanical stretch. However, the current results do not show any definitive trends or any conclusive data. Therefore, in the future, more experiments must be run, perhaps looking at other aspects such as cytokine response. This could provide a better overall picture and help explain why the trends observed in this study are present but are not significant.

REFERENCES

Gibson, Robert. "Clinical summary of visual impairment and intracranial pressure problem." *The Visual Impairment Intracranial Pressure Summit.* Houston, TX, 2011.

Hansen, H., Lagrèze, W., Krueger, O., & Helmke, K. (2011). Dependence of the optic nerve sheath diameter on acutely applied subarachnoidal pressure - an experimental ultrasound study. *Acta Ophthalmologica, 89*(6), 528-32.

Kramer, L. A., Sargsyan, A. E., Hasan, K. M., Polk, J. D., & Hamilton, D. R. (2012). Orbital and intracranial effects of microgravity: findings at 3-T MR imaging. *Radiology*, *263*(3), 819-827.

Marshall-Bowman, K. (2011). *Increased intracranial pressure and visual impairment associated with long-duration spaceflight* (Doctoral dissertation, NASA Johnson Space Center).

Nelson, E. S., Mulugeta, L., & Myers, J. G. (2014). Microgravity-Induced Fluid Shift and Ophthalmic Changes. *Life*, *4*(4), 621-665.

Winkler, M., Jester, B., Nien-Shy, C., Massei, S., Minckler, D. S., Jester, J. V., & Brown, D. J. (2010). High resolution three-dimensional reconstruction of the collagenous matrix of the human optic nerve head. *Brain research bulletin*, *81*(2), 339-348.

Figure:

Neuro-ophthalmology. (2015, October 3). Retrieved November 29, 2015, from http://clinicalgate.com/neuro-ophthalmology-2/